Hindawi
Journal of Control Science and Engineering
Volume 2023, Article ID 9760213, 1 page
https://doi.org/10.1155/2023/9760213

Retraction

Retracted: Application of Internet of Things Technology in the Construction of Bored Pile Foundation in a High Altitude Environment

Journal of Control Science and Engineering

Received 15 August 2023; Accepted 15 August 2023; Published 16 August 2023

This article has been retracted by Hindawi following an investigation undertaken by the publisher [1]. This investigation has uncovered evidence of one or more of the following indicators of systematic manipulation of the publication process:

(1) Discrepancies in scope

(2) Discrepancies in the description of the research reported

(3) Discrepancies between the availability of data and the research described

(4) Inappropriate citations

(5) Incoherent, meaningless and/or irrelevant content included in the article

(6) Peer-review manipulation

The presence of these indicators undermines our confidence in the integrity of the article's content and we cannot, therefore, vouch for its reliability. Please note that this notice is intended solely to alert readers that the content of this article is unreliable. We have not investigated whether authors were aware of or involved in the systematic manipulation of the publication process.

Wiley and Hindawi regrets that the usual quality checks did not identify these issues before publication and have since put additional measures in place to safeguard research integrity.

We wish to credit our own Research Integrity and Research Publishing teams and anonymous and named external researchers and research integrity experts for contributing to this investigation.

The corresponding author, as the representative of all authors, has been given the opportunity to register their agreement or disagreement to this retraction. We have kept a record of any response received.

References

[1] J. Liu, Y. Wang, Y. Guo, Z. Chen, and D. Jiao, "Application of Internet of Things Technology in the Construction of Bored Pile Foundation in a High Altitude Environment," *Journal of Control Science and Engineering*, vol. 2022, Article ID 4848447, 9 pages, 2022.

Hindawi
Journal of Control Science and Engineering
Volume 2022, Article ID 4848447, 9 pages
https://doi.org/10.1155/2022/4848447

Research Article

Application of Internet of Things Technology in the Construction of Bored Pile Foundation in a High Altitude Environment

Jiayin Liu, Yang Wang, Yingjun Guo, Zhipeng Chen, and Daowei Jiao

China Construction First Group The Fifth Construction Co., Ltd, Beijing 100000, China

Correspondence should be addressed to Yang Wang; 202009000063@hceb.edu.cn

Received 12 June 2022; Revised 1 July 2022; Accepted 11 July 2022; Published 31 July 2022

Academic Editor: Jackrit Suthakorn

In order to solve the problem that the current geophysical method is difficult to locate in the mud of bored piles, the problem of effective exploration of karst caves at the bottom of piles, the author puts forward the application of Internet of Things technology and sonar technology in the construction of bored pile foundation in a high altitude environment. Combined with the propagation characteristics of sonar stress waves, a sonar detection method for karst caves at the bottom of bored piles is proposed, and a sonar detector for karst caves at the bottom of piles (JL-SONAR) and signal analysis software (PBCA) are developed. The JL-SONAR detector realizes the emission and acquisition of onsite sonar signals, and the PBCA software completes the analysis and arrangement of the detection data. This technology makes full use of the mud conditions of bored piles, the development of karst caves within 10 m of the pile bottom can be tracked and detected in the process of hole formation, which has the advantages of low cost, high speed, and high precision. Experimental results show that Project A has been drilled in multiple directions at the bottom of the pile, the rock cores on the west side of the pile bottom are mostly fragmented, the rock quality index RQD is 15–30, and the quality of the foundation rock at the pile bottom is extremely poor, which verify the results of sonar detection. No slurry leakage occurred in Project B after drilling, and the cores were mostly short columns. The rock quality index RQD was 75 to 90, and the quality of the foundation rock at the bottom of the pile was good, which verifies the results of sonar detection. *Conclusion*. The research results provide a new solution for karst cave exploration in karst areas, especially in liquid environments.

1. Introduction

Frozen soil is very sensitive to temperature, the heat carried by concrete and the heat of hydration generated by cement hydration during the pouring of bored piles will cause the permafrost around the pile to heat up and melt, resulting in a decrease in its bearing capacity and freezing strength. In order to reduce the thermal disturbance of the frozen soil caused by the concrete pouring into the mould, the moulding temperature of the bored piles is generally controlled at about 5°C, which means that the pouring of the concrete can only be carried out at a lower temperature, and the surrounding area of the pile is frozen. Soil is its natural conservation environment [1]. After the pile foundation concrete is poured, heat is input to the frozen soil; as the frozen soil continues to freeze, the temperature in the concrete of the pile body gradually decreases, and finally the frozen soil returns to the original frozen state, and the pile body and the frozen soil around the pile reach a new thermal balance. Visible, the temperature field in the pile foundation concrete has the characteristics of being above 0°C for several days and continuously below 0°C in the later period. For the concrete of bored piles in the frozen soil area, the low temperature of entering the mold leads to the low curing temperature, which is not conducive to the formation of early strength of concrete, when the critical frost resistance of concrete cannot be formed early, frost crack damage of concrete will occur. On the other hand, concrete is a material with poor thermal conductivity, under the action of cement hydration heat, the highest temperature rise often occurs in the center of the pile concrete, after the concrete is poured, the surface concrete in contact with the permafrost

immediately inputs heat to the permafrost, which reduces its own temperature rapidly, which is likely to cause the temperature difference between the surface and the center of the pile foundation concrete to be too large, resulting in the formation of temperature cracks. At the same time, if the temperature of the concrete at the interface drops below 0°C in the plastic state, the water in the concrete pores will freeze and the ice crystals will expand and cause the pore structure to coarsen and deteriorate; it will also affect the durability of bored pile concrete [2]. The bored cast-in-place piles are buried in the frozen soil, which is a hidden project and is difficult to maintain; the concrete strength of the pile body is insufficient or the pores are deteriorated, this will leave the pile body with permanent and difficult to remove hazards, resulting in insufficient bearing capacity of the pile foundation, excessive settlement, and ultimately jeopardizing the safe operation of the bridge.

2. Literature Review

Suyuti et al. studied the phenomenon of hole expansion of pile foundation during construction; the phenomenon of hole expansion generally occurs when the groundwater is in a fluid state, the drill cone swings and floats greatly, and the indigenous loose layer is used, if several conditions are more serious, which can easily lead to the phenomenon of collapse. If the depth of the drilled hole meets the design and construction requirements, it is not necessary to carry out reaming. If the phenomenon of collapse occurs, the amount of concrete poured must be increased to ensure the quality of the pile foundation hole. If the hole wall continues to collapse, it shall be dealt with as a collapse accident [3]. Dakskobler et al. conducted research on foundation pit construction, the research shows that the use of foundation pit monitoring technology can ensure the safety of foundation pit construction and the surrounding construction environment to a certain extent; once problems occur, they can be found in time and can be effectively prevention of construction accidents. At the same time, by analyzing the test results, it can provide a certain reference value for the improvement and optimization of the construction method [4]. Ma et al. studied the load-bearing mechanism of bored piles, using the method of combining statistics with data models, and referring to a large number of experimental data after processing on the construction site, the method for judging the limit of superlong bored cast-in-situ piles and the advanced test method for carrying out the load test of large tonnage piles have been obtained, and the accuracy of the conclusions has been verified by engineering examples [5]. Cahyadi et al. studied the stress of the steel cage when the cast-in-place pile was poured with concrete and proposed that the quality of concrete, the speed of pouring concrete, the geological conditions of construction, and the human factors during construction are the main reasons for the floating of the steel cage and put forward targeted preventive measures, mainly including strict control of the concrete pouring speed, the quality of the concrete, the quality of the mud, and the rising speed of the conduit [6]. Mecozzi et al. studied the floating accident of the steel cage when pouring concrete, the research shows that the floating accident of the steel cage is mainly caused by improper operation during construction, for example, the reinforcement cage is not fixed firmly, the quality of concrete is poor, the lifting speed of the pipe is too fast, and the control of the buried depth of the pipe is not accurate; the measures adopted are to ensure the accurate and firm positioning of the steel cage, strictly control the lifting speed of the conduit, ensure the quality of the concrete, and control the embedding depth of the conduit. At the same time, the "barb" construction method can be used to jointly ensure the pile quality of poured concrete [7]. Ren et al. analyzed and discussed the floating of steel cages based on theoretical and practical experience and put forward relevant measures to prevent the floating of steel cages during construction of bored piles. The pouring speed of concrete, the distance from the conduit to the bottom of the hole, and the embedding depth of the conduit when pouring concrete, in order to a certain extent, the floating phenomenon of the steel cage can be avoided [8].

The author proposes a sonar detection method for karst caves at the bottom of bored piles and explores the application of sonar technology to the detection of karst caves at the bottom of piles, using the mud in the pile hole as the medium for the propagation and coupling of sound waves, in order to detect the development of karst caves at the bottom of the pile. Sonar technology was invented in 1906 and was first used in the military. After the 1970s and 1980s, sonar technology began to transform to civilian use and was mostly used in underwater positioning, sounding, etc. [9]. The author proposes a pile bottom karst cave sonar detection method, and on this basis, develops a pile bottom karst cave sonar detector (JL-SONAR) and signal analysis software (PBCA), and applies them to many projects; this method verifies the accuracy of the sonar detection method.

3. Research Methods

3.1. The Principle of the Sonar Detection Method of a Bored Pile Bottom Karst Cave

3.1.1. Sonar Detection Principle of a Pile Bottom Karst Cave. Sonar, in a narrow sense, refers to the method and equipment for judging the existence, location, and type of objects by using underwater sound waves. In a broad sense, any use of underwater sound waves as a communication medium, devices and methods to achieve a certain purpose are called sonar [10]. In the detection of karst caves at the bottom of bored piles, the author uses the sonar stress wave excited in the mud and water environment to detect the karst caves at the bottom of the pile.

Emission: The onsite host controls the sonar emission drive module through the communication cable, sends the electrical signal to the sonar emission transducer through the power amplifier, and converts it into a sound wave signal for vertical downward excitation in the mud environment of the bored pile bottom.

Propagation: Under the coupling action of the mud at the bottom of the pile, the acoustic impedance difference between the upper and lower media is effectively reduced,

the acoustic coupling rate is improved, and more sonar stress wave energy can smoothly enter the bedrock.

Reflection: After the sonar stress wave enters the bedrock and propagates downward, a significantly changed wave impedance surface is formed due to the karst cave at the bottom of the pile and the weak rock layer and the rock mass at the bottom of the pile, its physical properties are reflected in the density of rock or soil and the propagation velocity of elastic waves. Therefore, the transmission of the sonar stress wave from this interface will generate a strong reflection echo.

Receiving: Sonar reflected waves are received by sonar receiving transducers in 4 different directions around the sonar transmitting transducer. The azimuth angles of the four receiving transducers are measured by a three-dimensional electronic compass installed inside the probe [11]. The sonar reflected wave is converted into an electrical signal by the receiving transducer, and then is amplified, filtered and converted into a digital signal by the communication cable and transmitted to the on-site host for display and processing.

3.1.2. Analysis Principle of a Sonar Signal in the Pile Bottom Karst Cave. Since the distance between the sonar transmitting transducer and the receiving transducer is very small, it can be regarded as a very small offset. The reflected waveform is analyzed using one-dimensional wave theory.

The one-dimensional particle longitudinal vibration equation is the following formula:

$$\frac{\partial^2 u}{\partial t^2} = C^2 \frac{\partial^2 u}{\partial x^2}. \tag{1}$$

In the formula: u is the vibration position of the particle, t is the time, x is the direction of vibration, and C is the propagation velocity of the wave in the x direction.

The DAlembert solution is obtained as the following:

$$u(x,t) = f(x - Ct) + g(x + Ct). \tag{2}$$

It shows that the vibration of the particle is the superposition of two opposite traveling waves, if $f(x - Ct)$ is regarded as the initial down-going wave, then $g(x + Ct)$ is the reflected wave at the interface of different media at the bottom of the pile, they keep their original waveform and propagate and superimpose at the speed C. When a sonar stress wave propagates to the interface of media with different elastic properties, it will cause wave emission and refraction. At the same time, the reflection law satisfies two conditions: ① The stress on both sides of the interface must be equal and ② The velocity of the particle at the interface must be continuous. That is, the following formulas (3, 4):

$$P + P_R = P_T, \tag{3}$$

$$v + v_R = v_T. \tag{4}$$

In the formula: P, P_R, and P_T are the incident, reflected, and transmitted sound pressures, respectively; v, v_R, and v_T are the incident, reflected, and transmitted wave velocities, respectively.

$V = P/Z$, $Z = \rho C$ are known, and Z is the wave impedance of different media above and below the interface. We substitute it into formula (4) to obtain the following formula (5):

$$\frac{P}{Z_1} - \frac{P_R}{Z_1} = \frac{P_T}{Z_2}. \tag{5}$$

Simultaneous (3) and (5) can obtain the reflection coefficient as follows:

$$R = \frac{P_R}{P} = \frac{Z_2 - Z_1}{Z_1 + Z_2}. \tag{6}$$

The reflection coefficient R obtained from this can be used to analyze the wave impedance difference of each stratum at the bottom of the pile, so as to judge the completeness of the pile bottom, the existence of karst caves, the upper softness and the lower hardness, and the broken rock formation as shown in Table 1. The greater the absolute value of R, the greater the difference in wave impedance between the upper and lower media.

When the foundation rock at the bottom of the pile is complete, the time domain curve of the reflected wave received by the sonar probe at the bottom of the pile is ideally attenuated exponentially, the amplitude is attenuated uniformly, and no secondary reflection occurs, that is $R = 0$, and the signal energy is strong as shown in Figure 1.

When a karst cave is developed at the bottom of the pile, the wave impedance of the filling in the karst cave is smaller than that of the bedrock at the top of the karst cave, so the reflection coefficient is $R < 0$, the phase of the reflected wave is opposite to the reflected wave incident on the bottom of the pile, and the reflection on the time domain curve is the occurrence of secondary reflection, and an opposite-phase waveform is superimposed at the development of the karst cave as shown in Figure 2. When necessary, spectral analysis of the time-domain curve is required.

When the bottom of the pile encounters a harder rock layer, when the upper part is soft and the lower part is hard because the density of the lower layer medium is larger, its wave impedance is also larger, so the reflection coefficient $R > 0$ and the phase of the reflected wave at the interface is opposite to the reflected wave incident at the bottom of the pile, which is reflected in the time domain curve as a waveform with a positive phase superimposed at the interface as shown in Figure 3.

When the rock layer at the bottom of the pile is extremely broken, the bedrock at the bottom of the pile does not have a complete and clear radiation surface, and the received reflected signal is very weak compared with the signal when the bedrock is intact, that is, $R = 0$, and the signal energy is weak as shown in Figure 4.

3.2. Sonar Detection Device for the Bored Pile Bottom Karst Cave. According to the principle described in 3.1, the author developed a set of sonar detection device for the bored pile

Table 1: Analysis of the sonar reflection signal at the bottom of the pile.

Reflection coefficient R > 0	Reflection coefficient $R > 0$	Reflection coefficient $R = 0$ and the signal energy is strong	Reflection coefficient $R = 0$ and weak signal energy
The bedrock is soft and hard	There is a cave at the bottom of the pile	Bedrock intact	Bedrock broken

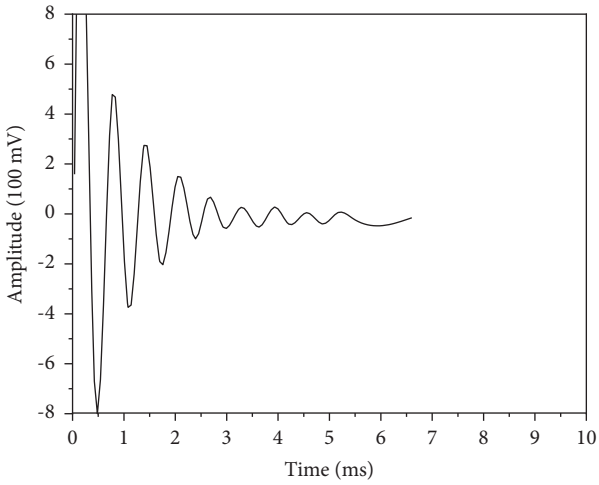

Figure 1: The ideal reflected signal when the pile bottom is complete.

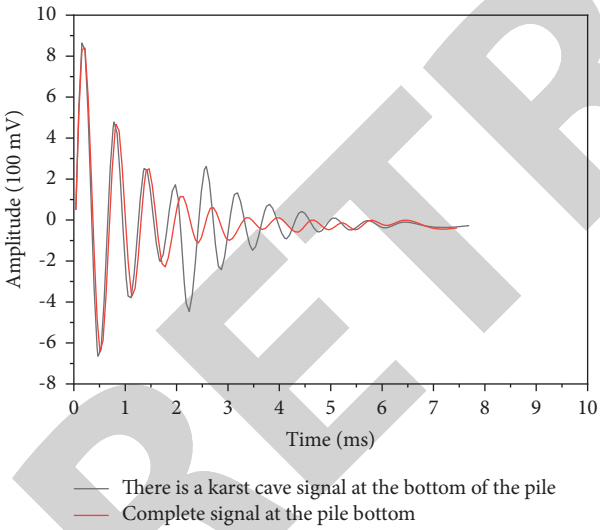

Figure 2: The ideal reflection signal when there is a karst cave at the bottom of the pile.

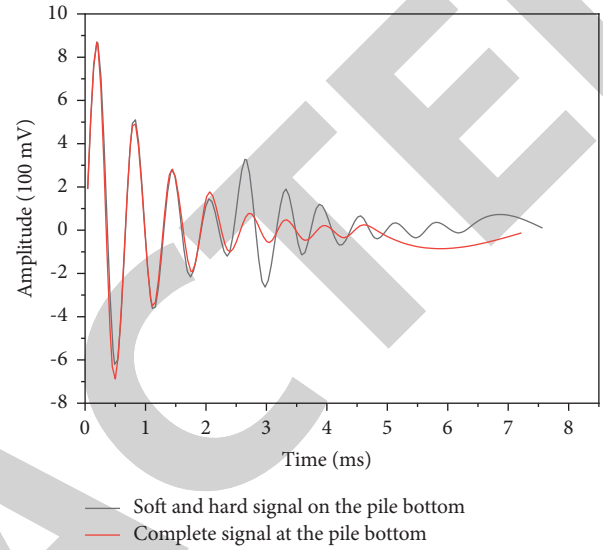

Figure 3: Ideal reflected signal with soft top and bottom hard bottom.

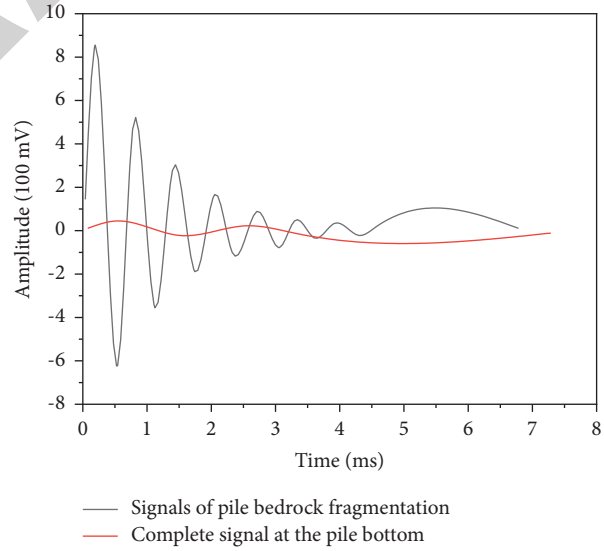

Figure 4: The ideal reflection signal when the foundation rock at the bottom of the pile is extremely broken.

bottom karst cave, mainly including pile bottom sonar detector (JL-SONAR) and sonar signal analysis software (PBCA).

3.2.1. Pile Bottom Karst Cave Sonar Detector JL-SONAR. The developed pile bottom karst cave sonar detector (JL-SONAR) includes an onsite host set on the surface of the pile hole, a sonar detection probe set at the bottom of the pile hole, and a communication cable set between the host and the sonar detection probe [12]. The structure of the sonar detector for the karst cave at the bottom of the pile is shown in Figure 5.

As shown in Figure 5, the detector is mainly composed of the onsite host and the sonar probe. The onsite host mainly includes the central processing unit, human-computer interaction equipment, and memory; The sonar probe mainly includes a sonar transmitting transducer and a sonar receiving transducer.

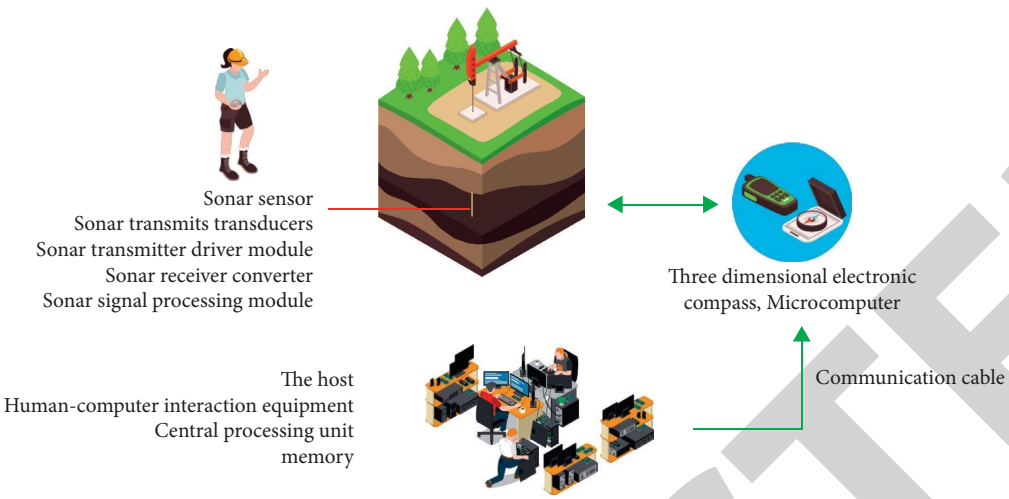

Figure 5: Structure block diagram of a sonar detector for the karst cave at the bottom of pile.

The human-computer interaction device in the host realizes the input and output of instructions. The central processing unit mainly completes the processing of input instructions, generates corresponding operation control signals, guides the work of the sonar probe, and completes the calculation of sonar detection data. The memory completes the storage of sonar detection data.

The sonar probe includes a microcomputer, a three-dimensional electronic compass, a sonar transmitting device, and a sonar receiving device. The microcomputer realizes the control and transmission of the instructions of each device and realizes the information handover with the onsite host. The three-dimensional electronic compass is installed horizontally in the sonar probe shell, and the north-pointing direction of the compass points to the installation direction of the sonar receiving transducer [13]. The sonar transmitting device includes a sonar transmitting transducer and a corresponding driving module. The sonar receiving device includes a sonar receiving transducer and a processing module, generally, 4 to 8 groups of receiving devices are placed around the transmitting device.

The sonar transmitting transducer (−5–1) and the sonar receiving transducer (−5–2) developed by the author have parameters shown in Tables 2 and 3.

As shown in Table 2, the transmitting power of the transmitting transducer reaches 10 kW, and the transmitting frequency band is 200 Hz to 8 kHz. The high-frequency determines the high detection accuracy, and the high-power and wide-band sonar emission, the rapid attenuation of the high-frequency part is avoided, and the recognizability of the signal is greatly improved.

When transmitting a signal, the human-computer interaction device sends out a sonar stress wave transmitting command. After the instruction is transmitted to the microcomputer in the sonar probe, the microcomputer controls the sonar transducer to convert the electrical signal into an acoustic signal through the sonar emission drive module and emits the sonar stress wave.

When receiving signals, 4 to 8 sonar-receiving transducers around the transmitting probe simultaneously convert the received acoustic signals into electrical signals, and the signals are transmitted to the microcomputer through the sonar signal processing module [14]. The sonar signal processing module is composed of digital circuits, completing the preprocessing of the received signal. Finally, the microcomputer collects the multichannel processed digital signal, transmits it to the on-site host through the communication cable for processing and analysis, and completes the storage and output of the data.

3.2.2. Signal Analysis Software PBCA. The pile bottom karst cave sonar detector analysis software PBCA developed by the author is a waveform analysis software matched with the pile bottom karst cave sonar detector JL-SONAR. The PBCA program development environment adopts Microsoft Visual Studio 2008 and uses C# as the programming language, its operating environment is Windows, which can be installed on the onsite host for onsite analysis, or can be analyzed on the PC after work.

PBCA signal analysis software is mainly composed of an input module, wave profile display and transformation module, signal processing module, labeling module, and output module.

The input module realizes the writing of sonar signals, the original detection file data of the same pile in different directions can be integrated, and up to 12 sonar signals of different angles of receiving transducers can be written at the same time.

The wave profile display and transformation module realizes the sonar signals of different channels, composes stress wave profiles in the order of their azimuth angles, completes time-depth conversion, and restores the true amplitude of waveform data, that is, exponential amplification of the original waveform [15]. Moreover, we realize the contrast display of the original waveform and the processed waveform of the single-channel sonar signal.

The signal processing block provides several ways to process raw waveforms:

Table 2: Parameters of a sonar transmitting transducer.

Model	Transmit frequency	Maximum instantaneous power/kW	Signal consistency	Sonar spread angle/(°)
JL–5–1	200 Hz ~ 8 kHz	10	Good	More than the 120
Features	Operating temperature/°C	Way of working	Pressure/MPa	Operating voltage/V
High energy, broadband, short aftershocks	−40 ~ +80	Single, continuous	1.0	12

Table 3: Sonar-receiving transducer parameters.

Model	Resonant frequency/kHz	Usage frequency	Capacitance	Sensitivity/dB
JL–5–2	30 ± 2	100 Hz ~ 10 kHz	1 600 pF ± 20%	−190
Minimum impedance	Operating temperature/°C	Pressure/MPa	Shell material	Use
400 Ω ± 20%	−40 ~ +80	1.0	Can be used in weak acid and weak alkali environment	Sonar monitoring

(1) Parametric filtering: First, we perform Fourier transform on the signal, do spectrum analysis, remove high-frequency and low-frequency interference waves, and analyze the real and effective frequency band signal by selecting an appropriate filtering range;

(2) Differential signal: When the reflection is not obvious, differential processing is performed on the signal to amplify the degree of waveform distortion;

(3) Integral signal: We integrate the signal to properly reduce aftershocks;

(4) Reflection extraction: Based on the estimation of the phase difference of the same signal at different sampling times, selecting an appropriate reflection coefficient can clearly show the phase mutation of the waveform [16]. The labeling module realizes manual labeling of karst caves, fissures, abnormal location shapes, or interfaces. The output module implements interfaces with other applications and can automatically save reports in Excel format.

3.3. Onsite Detection Implementation Method. The pile bottom karst cave is divided into the following steps when on-site:

(1) Place the probe: We use the orifice bracket through the communication cable to place the sonar detection probe at the bottom of the pile, and connect it with the on-site host through the communication cable. When there is no mud or water at the bottom of the artificially dug pile, 10–20 cm of water should be poured in to ensure that the sonar transmitter and sonar sensor of the sonar probe can be in contact with the water, so that the sonar stress wave can be connected to the pile. Bottom interface coupling.

(2) Probe leveling: The field host uses the three-dimensional compass in the probe, reads the attitude of the sonar detection probe at the bottom of the pile and the orientation of each sonar receiving sensor through the communication cable, and makes sure the sonar transmitting transducer is nearly vertical to the bottom of the pile.

(3) Pile bottom detection: When the sonar detection probe is placed, the onsite host controls the sonar emission drive module and the sonar transmitter to transmit sonar stress waves through the communication cable, controls the sonar signal processing module to receive the sonar signal, and digitizes the received sonar signal; the data are transmitted to the onsite host for display and processing through the communication port of the single-chip microcomputer by the communication cable.

(4) Multi-angle detection: After the current detection data are detected, the sonar transmitting transducer can be rotated along with the receiving sensor in a certain direction, and then we repeat steps (2) and (3) and perform 2 detections again to obtain a total of 3 groups. Signals in 12 directions.

(5) Software analysis: Using the analysis software PBCA of the pile bottom karst cave sonar detector, all the detected sonar received signals are arranged in the azimuth order of the sonar receiving sensors to generate the detection sonar stress wave profile, and comprehensive processing and analysis are carried out. The development of karst caves within 10 m of the pile bottom is obtained, which meets the specification, and it is determined that there are no karst caves or weak rock masses within the range of 3 times the pile diameter of the pile bottom and not less than 5 m.

4. Analysis of Results

4.1. A Commercial Engineering Example

4.1.1. Project Overview. A commercial engineering project is proposed to build the main building with a height of 48

floors and a height of 150 m, with two floors of basements and two floors of shops along the street on the north and east sides. The proposed building is proposed to adopt a shear wall structure. The landform area of the site belongs to the sloping landform of the dissolution remnant peaks, and the local topography fluctuates greatly.

According to the survey and drilling data, the underlying bedrock of the site is a soluble carbonate limestone, and the karst forms are mainly karst caves, troughs, and karst pores. The karst burial depth and scale vary within the exploration depth range, and the burial depth is 19.10–32.50 m. The cave height is 0.90–1.70 m, among the 79 exploration holes drilled into the limestone, 4 exploration holes have exposed 4 karst caves with different buried depths and cave scales, and the rate of encountering caves is 5.33%. 622.6 m, the total cumulative height of the cave is 5.30 m, the linear karst rate is 0.85%, the regularity of karst development is not strong, and it belongs to the site with weak karst development; There is local dissolution in the limestone (broken) and limestone (complete) layers [17]. Groundwater exists in the site within the exploration depth range, and karst still has a trend of further development under the action of groundwater.

Based on the above karst characteristics, the proposed site is a site with weak karst development, the regularity of karst development is not strong, the local overlying soil layer is thin, and the karst cave has a great impact on the foundation engineering of high-rise buildings, so pile foundation treatment is adopted.

4.1.2. Pile Bottom Karst Cave Detection Map. In the 1-1 to 1–3 floors of the project, the pile bottom karst cave detection signal with the pile hole number 461. The azimuthal angle of the pile bottom is 338° ~ 106°, and there is a secondary reflection signal of the negative phase of the karst cave at about 2 m at the pile bottom, that is, $R < 0$. After further drilling in this direction at the bottom of the pile, the mud in the hole obviously leaked. This phenomenon verifies the result of sonar detection, and there is a karst cave on the north side of the pile bottom. The karst cave is gradually penetrated by the method of short stroke and fast frequency impact onsite. When the roof of the karst cave is broken down, the mud is immediately added to the hole, the drilling is lifted to the orifice, and schist, clay blocks and cement are put into the hole to fill the karst cave. When the internal water head is stable, the construction will be continued after the protective wall is formed in the area of the karst cave.

In the 1-1 to 1–3 floors of the project, the pile bottom karst cave detection signal with the pile hole number 477. The reflected wave signal on the east side of the pile bottom is strong, no obvious secondary reflection is found, and the bedrock is relatively complete. However, the reflected signal from the west surface of the pile bottom is very weak. Even if the set amplitude amplification factor is increased, it is difficult to see the obvious reflected signal, that is, $R = 0$, and the signal energy is weak. Therefore, it can be judged that the bedrock on the west side is extremely broken, and the energy loss of the sonar stress wave is very large. After drilling in multiple directions at the bottom of the pile, the rock core on the west side of the bottom of the pile is mostly fragmented, and the rock quality index RQD is 15 to 30. According to Table 4, the quality of the foundation rock at the bottom of the pile is extremely poor, which verifies the results of the sonar detection. The site is treated by continuing the percussion drilling to the complete bedrock surface.

4.2. Example of B Project

4.2.1. Project Overview. Project B is proposed to build 1#~5# logistics warehouses and office buildings, 5~12 stories high, frame shear structure, and column foundations are planned, the construction site is located in Pingba Town, Anshun City, Guizhou Province; the site is located in the complex tectonic deformation area of Zunyi fault arch in Guiyang, Qianbei Tailong, in the Yangtze quasi-platform; there are no faults and folds in the area, and the geological structure is of a simple type, according to the ground investigation of the site and the analysis of the drilling data, there is no fault passing through the proposed site, the underlying bedrock is a monoclinic structure, and the stratum occurrence is 160° < 20°. The surface of the site is brown-yellow pigment filling and slope clay, and the underlying bedrock is medium-thick layered dolomite of the Lower Triassic Anshun Formation.

Among the 47 drilled holes, 11 encountered karst caves, with a rate of 23.4% of the holes encountered. The height difference of the bedrock surface is 0.8–3.5 m, which belongs to the middle-developed area of karst. The depth of the exposed karst cave in this site is 3.9–9.5 m, the vertical height of the karst cave is generally 0.5–2.5 m, and the largest is 4.7 m; the proposed building has a large load and a large underground water depth, the designed foundation depth is less than 0.5 m from the bottom of the cave.

4.2.2. Pile Bottom Karst Cave Detection. The detection signal of the karst cave at the pile bottom with the pile number 3–2 in the 3# warehouse can be seen from the bold part of the waveform in the figure. There is an obvious negative phase secondary reflection signal of the karst cave at 2 m below the east of the pile bottom, that is, $R < 0$. After further drilling at the bottom of the pile, due to the existence of the karst cave at the bottom of the pile, the mud in the hole has an obvious leakage phenomenon, which verifies the result of the sonar detection; there are karst caves in the east of the pile bottom [18]. After the onsite breakdown of the karst cave roof, it was found that the height of the karst cave was about 1 m; first, the rubble, sand mixture, and cement slurry were thrown and filled, and then the rubble was extruded with small strokes to form the outer protective wall of mud and gravel, and the impact was continued after the protective wall reached its strength, through the cave [19]. In the 3# warehouse, the pile bottom karst cave detection signal with the pile number 3–12, the pile bottom reflected wave signal is attenuated evenly, and there is no obvious secondary reflection, that is, $R = 0$, and the signal energy is strong, it can be determined that the foundation rock at the bottom of the pile is complete, and there are no adverse geological

Table 4: Rock quality evaluation criteria.

Rock quality index (RQD) value	Rock quality evaluation
> 90	It is good
75 ~ 90	Better
50 ~ 75	Poor
25 ~ 50	Difference
< 25	Very poor

phenomena such as karst caves and fractures. There is no leakage of slurry after drilling, the core is mostly short column, and the rock quality index RQD is 75–90. According to Table 4, the quality of the foundation rock at the bottom of the pile is good, which verifies the results of sonar detection [20, 21].

5. Conclusion

Through the development and application of the sonar detection method for karst caves at the pile bottom, it is believed that the advantages of the sonar detection method applied to the detection of karst caves at the bottom of bored piles are as follows:

(1) Sonar technology makes good use of mud, a material whose acoustic impedance is closer to bedrock, as a coupling medium, which effectively reduces the acoustic impedance difference between the upper and lower media; thus, the acoustic coupling rate is improved, so that the acoustic waves can be smoothly introduced into the foundation rock at the bottom of the pile. The existence of mud creates technical obstacles to other exploration methods, and the sonar detection method cleverly turns this disadvantage of a mud environment into an advantage.

(2) The detection results are not affected by the filling in the cave. Regardless of whether there is a filler in the cave, the wave impedance of the air, water, clay, and other substances in the cave is much smaller than that of the bedrock on the roof of the cave, so the superimposed phase of the reflected wave will be opposite to the incident wave, and the test signal consistency is very strong.

(3) The accuracy of detecting karst caves is high, and the smallest karst caves with a size of 10 cm can be detected. The resolution of acoustic detection increases with the increase of the frequency of the acoustic wave, but during the propagation of the acoustic wave, the high-frequency part will attenuate before the low frequency. In order to protect the high-frequency part of the signal, it is necessary: ① The transmission frequency range is wide and ② the transmitted signal energy is strong. The source frequency band developed by the author is 200–8 000 Hz, and the power reaches 10 kW, while emitting high-frequency sound waves, the broadband and high-power source effectively protects the high-frequency part of the signal and improves the resolution of the waveform.

(4) Detection does not depend on advance drilling, it is a method of rapid nondestructive testing, which can complete the general inspection of each pile. The time to detect a pile on-site is within 10 minutes, and the tracking and detection of the karst cave at the bottom of the pile can be carried out at any time with the progress of the hole formation. It brings great convenience and operability to the quality inspection of the foundation rock at the pile bottom, which makes the technology easy to be popularized.

Data Availability

The data used to support the findings of this study are available from the corresponding author upon request.

Conflicts of Interest

The authors declare that they have no conflicts of interest.

References

[1] H. T. Santoso and J. Hartono, "Comparative analysis of the bearing capacity of the pile foundation based on the results of the SPT test and dynamic testing," *Civil Engineering Research Journal*, vol. 4, no. 1, pp. 30–38, 2020.

[2] R. Daher and J. M Abbas, "The behavior of pile group under inclined static load with different angle of inclination in sandy soil," *Diyala Journal of Engineering Sciences*, vol. 14, no. 2, pp. 52–61, 2021.

[3] S. Suyuti, Z. K. Misbah, and M. A. Sultan, "Bearing capacity of soil bags on soft ground reinforced by bamboo pile," *International Journal of Geomate*, vol. 16, no. 53, pp. 32–39, 2019.

[4] I. Dakskobler and L. Poldini, "Phytosociological analysis of noble hardwood forests (ostryo-tilienion platyphylli) in the karst and its neighbouring regions (sw Slovenia)," *Hacquetia*, vol. 20, no. 2, pp. 327–372, 2021.

[5] H. H. Ma, M. Peng, F. Guo et al., "Factors affecting the translocation and accumulation of cadmium in a soil-crop system in a typical karst area of guangxi Province, China," *Huan Jing Ke Xue*, vol. 42, no. 3, pp. 1514–1522, 2021.

[6] A. Cahyadi, H. Reinhart, A. Wahyu Ristiawan et al., "Hydrogeology of mangsri cave, gunungsewu karst area, java island, Indonesia," *Sumatra Journal of Disaster Geography and Geography Education*, vol. 5, no. 1, pp. 1–6, 2021.

[7] B. Mecozzi, L. Bellucci, F. Giustini, A. Iannucci, and R. Sardella, "A reappraisal of the pleistocene mammals from the karst infilling deposits of the maglie area (lecce, apulia, southern Italy)," *Italian Journal of Paleontology and Stratigraphy*, vol. 127, no. 2, pp. 355–382, 2021.

[8] K. Ren, X. D. Pan, J. P. Liang, C. Peng, and J. Zeng, "Sources and fate of nitrate in groundwater in a typical karst basin: insights from carbon, nitrogen, and oxygen isotopes," *Huan jing ke xue= Huanjing kexue/[bian ji, Zhongguo ke xue yuan huan jing ke xue wei yuan hui "Huan jing ke xue"*, vol. 42, no. 5, pp. 2268–2275, 2021.

[9] P. Esmaili, F. Cavedo, and M. Norgia, "Characterization of pressure sensor for liquid-level measurement in sloshing condition," *IEEE Transactions on Instrumentation and Measurement*, vol. 69, no. 7, pp. 4379–4386, 2020.

[10] F. Xue, M. Cai, T. Wang, and T. Zhao, "Characteristics of karst cave development in urban karst area and its effect on the stability of subway tunnel construction," *Advances in Civil Engineering*, vol. 2021, Article ID 8894713, 12 pages, 2021.

[11] G. Zhang, K. Bashiri, M. Kneteman et al., "Seroprevalence of human betaretrovirus surface protein antibodies in patients with breast cancer and liver disease," *Journal of Oncology*, vol. 2020, Article ID 8958192, 9 pages, 2020.

[12] A. T. Cave, S. A. Lowenstein, C. Mcbride, J. Michaud, E. J. Madriago, and C. Ronai, "Pulse oximetry screening and critical congenital heart disease in the state of Oregon," *Clinical Pediatrics*, vol. 60, pp. 290–297, 2021.

[13] R. Walters and N. Zupan Hajna, "3D laser scanning of the natural caves: example of Škocjanske jame," *Geodetic Journal*, vol. 64, pp. 89–103, 2020.

[14] P. Tueller, R. Kastner, and R. Diamant, "Target detection using features for sonar images," *IET Radar, Sonar & Navigation*, vol. 14, no. 12, pp. 1940–1949, 2020.

[15] D. Syamsuddin, D. Satria Muyadi, and A. Prasetia Adi, "Interpretation of seabed objects based on backscatter values using a side scan sonar instrument (case study of the Pertamina pipe in Balongan)," *Datum Chart Journal*, vol. 6, no. 1, pp. 52–68, 2021.

[16] L. Character, A. Ortiz JR, T. Beach, S. Luzzadder-Beach, and S. Luzzadder-Beach, "Archaeologic machine learning for shipwreck detection using lidar and sonar," *Remote Sensing*, vol. 13, no. 9, pp. 1759–1778, 2021.

[17] C. Liu, M. Lin, H. L. Rauf, and S. S. Shareef, "Parameter simulation of multidimensional urban landscape design based on nonlinear theory," *Nonlinear Engineering*, vol. 10, no. 1, pp. 583–591, 2021.

[18] R. Huang, S. Zhang, W. Zhang, and X. Yang, "Progress of zinc oxide-based nanocomposites in the textile industry," *IET Collaborative Intelligent Manufacturing*, vol. 3, no. 3, pp. 281–289, 2021.

[19] C. Jiayao, B. Jianqi, L. Xin, A. Wenye, Z. Jing, and C. Fangchuan, "Degradation of toluene in surface dielectric barrier discharge (sdbd) reactor with mesh electrode: synergistic effect of uv and tio 2 deposited on electrode," *Chemosphere*, vol. 288, 2021.

[20] S. Shriram, B. Nagaraj, J. Jaya, S. Shankar, and P. Ajay, "Deep learning-based real-time AI virtual mouse system using computer vision to avoid COVID-19 spread," *Journal of Healthcare Engineering*, vol. 2021, Article ID 8133076, 8 pages, 2021.

[21] N. Yuvaraj, K. Srihari, G. Dhiman et al., "Nature-inspired-based approach for automated cyberbullying classification on multimedia social networking," *Mathematical Problems in Engineering*, vol. 2021, pp. 1–12, Article ID 6644652, 2021.